Electromagnetic Compatible Energy Measurements Using the Orthogonality of Nonfundamental Power Components

Tom Hartman, Roelof Grootjans, Niek Moonen, *Member, IEEE*, and Frank Leferink, *Fellow, IEEE*

***Abstract*—Measurement bandwidth of energy measurements are increasing to incorporate all the harmonics created by nonlinear loads and distributed generators making the measurement electronics complex and sensitive to electromagnetic interference. This article proposes to change the accuracy paradigm by focusing on fundamental active power and lower harmonics for energy metering, simplifying the electronics and making them robust against electromagnetic interference. Using the orthogonality of power flow via Parseval's theorem, a theoretical analysis, simulations, and measurements on power calculations using the fundamental active power are presented. It is shown that a perfect power measurement is achieved with a pure 50 Hz supply voltage, regardless of the nonlinear current. Even with the highest allowed harmonic distortion of the voltage and the current as listed in the international standards EN 50160 and IEC 61000-3-2, more than 97.5% of the active power is contained in the fundamental active power. Negligible active power is contained in the higher frequency components. This error margin falls within limits for electricity meters. Filtering the current with a basic low-pass filter can prevent the erroneous measurements that have appeared with static energy meters. In other words, it has been proven that negligible energy flows in the higher frequency components.**

***Index Terms*—Conducted immunity and emissions, EMC measurements, low frequency EMC, power electronics, power quality.**

I. Introduction

THE POWER and energy metering is conventionally focused on the phase deviation between supply voltage and loading currents. All traditional loads could be considered to be of a linear nature with some degree of capacitive or inductive behavior. With the introduction of semiconductor devices loads became inherently nonlinear and thus started introducing harmonic distortions [1]–[3]. This is now a classical electromagnetic interference (EMI) phenomenon that raises (PQ) issues. Over the last decades, the silicon-based metal oxide semiconductor field effect transistor (MOSFET) and insulated-gate bipolar transistor (IGBT) have been pushed to the limit of their physical operating boundaries, by increasing switching speeds, decreasing physical sizes while increasing power densities. This has been pushed even further by implementing several new technologies based on wide bandgap materials, like Galium-Nitride (GaN) and Silicium-Carbide (SiC), or any hybrid form, increasing the high frequency spectral content of the switching waveforms [4].

Conducted EMI in the grid has been extensively investigated over the years [1], [5], [6]. For instance, harmonic current flow in a three-phased system, which causes heating or in extreme cases even burning out of the conductor [7], [8]. Harmonic voltages and currents are conventionally measured up to 2 kHz, and EMI measurements for PQ, mainly voltage, are described in [9]. The standardization community shows an increased interest in the frequency range between 2 and 150 kHz developing standards for apparatus [10]. This together with more accurate, faster, and cheaper measurement equipment results in a trend in power analysis, and inherently energy metering, to increase the measurement frequency bandwidth to solve metering issues attributed to EMI [11]–[13].

Household energy metering has been proven to be susceptible to EMI [14]–[18]. In [14], it was shown that static energy meters with a Rogowski coil current sensor showed positive deviations and static energy meters with a Hall effect current sensor showed negative deviations. Relative energy measurement errors of up to 581% were shown in [15]. In [16], a current gradient of $1.1\ A/\mu s$ was shown to cause large metering errors. In [17], an energy measurement error of 2675% for a commercial of the shelf (COTS) water pump was shown and in [18] sensitivity of static energy meters due to changes in nonsinusoidal load conditions was shown.

The IEC 61000-4-19 standard [19], to which all the static and smart meters have to adhere, was updated in 2014, after negative energy metering errors had been shown to exist. However, energy meters compliant with the tests described in [19] are also showing the higher meter readings [14]–[18], [20], [21]. It has been identified that currents containing a high $\frac{di}{dt}$ are more problematic for derivative current sensing elements [21]. The common approach of measuring the current components up to high frequencies does not contribute to a better energy meter reading, because of the orthogonality of the fundamental voltage

Manuscript received May 15, 2020; revised July 23, 2020; accepted August 20, 2020. Date of publication September 18, 2020; date of current version April 14, 2021. This work was supported by the EMPIR programme cofinanced by the Participating States and from the European Union's Horizon 2020 research and innovation programme. *(Corresponding author: Tom Hartman.)*

Tom Hartman, Roelof Grootjans, and Niek Moonen are with the University of Twente, 7522NB Enschede, The Netherlands (e-mail: tom.hartman@utwente.nl; r.grootjans@utwente.nl; d.j.g.moonen@utwente.nl).

Frank Leferink is with the University of Twente, 7522NB Enschede, The Netherlands, and also with the THALES Nederland B.V., 7554 RR Hengelo, The Netherlands (e-mail: leferink@ieee.org).

Color versions of one or more of the figures in this article are available online at https://ieeexplore.ieee.org.

Digital Object Identifier 10.1109/TEMC.2020.3019974

frequency and the higher current harmonics. In this article, a theoretical derivation is given to why only frequencies coexisting in both the voltage and current waveforms are of interest for active power calculations. The theoretical analysis results are substantiated with simulations and measurement results of ideal sinusoidal voltage waveforms combined with nonsinusoidal currents. Also, the effect of distorted voltage waveforms on the active power measurements have been analyzed, up to the maximum voltage distortion limit described in EN50160 [22] and the current distortion limit described in IEC 61000-3-2 [23].

The theoretical analysis is based on Parseval's theorem and is consistent with the theory of orthogonal power flow presented in [24], which states that power produced by different frequency components is orthogonal to each other. To verify the presented theory and simulation results, measurements have been performed using first, a dc power supply to demonstrate that measurements of the active power can be limited to the frequencies of the voltage supplied. The effect of placing filtering elements in the measurement circuit to decrease the susceptibility to EMI and thus increase electromagnetic compatibility (EMC) levels is investigated. The practical implementation of such a filter is, however, outside the scope of this article. This section is followed by a more practical and commonly seen power system that uses the 50 Hz as the fundamental supplying voltage component, first perfectly sinusoidal and afterward distorted with higher harmonics. The active power is calculated via both the time and frequency domain for better insights in the orthogonality of the power calculation.

The rest of this article is organized as follows. In Section II, the theory of orthogonal power flow is presented based on Parseval's theorem. In Section III simulation results are presented showing the ratio of the fundamental active power with respect to the total power over a range of total harmonic distortion (THD) values for both the voltage and the current. Sections IV–VI show the active power measurement results of an ideal dc, ideal 50 Hz, and distorted 50 Hz voltage source, respectively. Section VII provides the overview of this article and, finally, Section VIII concludes this article.

II. Theoretical Background—Orthogonality

The Parseval's theorem in its most general form, known as Plancherel's theorem, will be used to show the orthogonality of power for the current and the voltage. Parseval shows that a multiplication in the time domain within an integral stays a multiplication in the frequency domain within an integral, under the following circumstances shown in (1).

$$\int_{-\infty}^{\infty} f(x)\cdot g^{*}(x)dx = \int_{-\infty}^{\infty} F(\xi)\cdot G^{*}(\xi)d\xi \tag{1}$$

where $f(x)$ and $g(x)$ can be mathematical relations in the time domain and $F(\xi)$ and $G(\xi)$ are their Fourier transforms, respectively. This theorem can be used for the equation of the average power, which follows from the instantaneous power:

$$P_{\text{av}} = \frac{1}{2T}\int_{-T}^{T} i(t)\cdot v(t)dt \tag{2}$$

where (2) equals the circumstances for the left side in (1), if we include a rectangular function to incorporate for the impossible infinite measurement time as follows:

$$P_{\text{av}} = \frac{1}{2T}\int_{-\infty}^{\infty} i_T(t)\cdot v(t)dt \tag{3}$$

where $i_T(t) = i(t)\cdot g(t)$ and $g(t) = \text{rect}(\frac{t}{2T})$. From (3) and Parseval's theorem, it is concluded that

$$P_{\text{av}} = \frac{1}{2T}\int_{-\infty}^{\infty} I_T(f)\cdot V(f)df \tag{4}$$

where $I_T(f) = I(f) * 2T\text{sinc}(2Tf)$, which causes spreading in the frequency domain due to the limited measurement time. Equation (4) shows that to calculate the average power individual frequency components in the voltage are only multiplied by the corresponding frequency component in the current. If the voltage is assumed to be a pure 50 Hz sinusoidal waveform, $A_v\cos(2\pi f_c t)$, (4) transforms into

$$P_{\text{av}} = \frac{1}{2T}\int_{-\infty}^{\infty} I_T(f)\cdot\frac{A_v}{2}[\delta(f-f_c)+\delta(f+f_c)]df. \tag{5}$$

After which, (5) simplifies into

$$P_{\text{av}} = \frac{A_v}{4T}[I_T(f_c)+I_T(-f_c)] \tag{6}$$

where the convolution in $I_T(f)$ has to be performed first after which, it can be considered at $f = f_c$.

Equation (6) shows that only the fundamental active power has to be considered, regardless of the THD_I. This means that frequency components in the current, other than the main 50 Hz component, only influence the active power calculation at 50 Hz due to the spreading in the frequency domain, which can be attributed to the limited measurement time [25], [26]. This influence can be quantified by considering the envelope function of the sinc, which decreases linearly with $1/(2T\Delta f)$. The fact that only the 50 Hz fundamental current component is needed for accurate active power and energy measurements are always valid for an ideal power supply grid, allowing for highly accurate measurements. This allows for filtering elements to be placed in the measurement circuit to decrease the susceptibility to EMI. It is suggested that the designer creates a filter with a fast roll-off while keeping the amplitude of the fundamental unaffected. Also, the phase shift introduced by the filter should be kept as small as possible. In actual systems, the grid has some impedance, and the distorted current consumption will result in voltage distortion. As the energy supplier is responsible for the THD_v, the energy supplier is able to minimize any energy measurement errors by reducing the THD_v. This effect has been included in the analysis as well.

III. Simulation

To demonstrate the effect of orthogonal power flow, which shows that with an ideal 50 Hz grid only the fundamental frequency component of the current has to be considered regardless of the THD_I, a simulation has been performed. The effect of different THD values in both the current and the voltage on the

TABLE I
EN 50160 HARMONIC VOLTAGE LIMITS

Odd Harmonics				Even Harmonics	
Order	U_n [%]	Order	U_n [%]	Order	U_n [%]
5	6.0	3	5.0	2	2.0
7	5.0	9	1.5	4	1.0
11	3.5	15, 21	0.5	6 ... 24	0.5
13	3.0				
17	2.0				
19, 23, 25	1.5				

TABLE II
CURRENT LIMITS FOR CLASS C EQUIPMENT

Harmonic order n	Harmonic current w.r.t. the fundamental frequency [%]
2	2
3	$30{\cdot}\lambda^*$
5	10
7	7
9	5
$11 \leq n \leq 39$ (odd n only)	3
$^*\lambda$ is the circuit power factor	

total active power will be presented. Both a linear load and a nonlinear load will be examined.

For the maximum harmonic distortion of the voltage the EN 50160 standard for voltage characteristics of electricity supplied by public distribution networks is used as reference [22]. For a linear load, the same harmonics will be present for the current. The maximum voltage harmonics are shown as Table I. In the situation of a nonlinear load, the effect of Class C equipment is used as reference, based on the International Standard IEC 61000-3-2 [23]. This standard prescribes the maximum value for harmonic currents from the second harmonic up to and including the 40th harmonic. IEC 61000-3-2 applies to equipment with a rated current up to 16 A. The standard established four groups of equipment, each with their own harmonic emission limit. Class A consists of household appliances, tools, and audio equipment, Class B holds portable tools and arc welding equipment, which is not professional. Class C is specified for lighting equipment, including dimmers. Class D is for personal computers and television receivers consuming less than or equal to 600 W. The standard of Class C equipment has its limits specified as a percentage of the fundamental frequency as does the EN 50160 standard. For this reason and for creating a generic case, by not specifying a specific amplitude for the fundamental frequency, the limits for Class C equipment were chosen as an example. In actual households, the type of appliances differ, and the diversity will result in an overall lower THD_I, compared to one of the classes only [7]. An overview of the specified current harmonics for Class C equipment is shown in Table II.

The THD is defined with respect to the fundamental as shown in (7).

$$\text{THD}_V = \sqrt{\sum_{n=2}^{\infty} \frac{V_n^2}{V_1^2}} \tag{7}$$

where V_n represents frequency components that are integer multiples of the fundamental frequency. Equation 7 shows the THD_V, but the same concept holds for the THD_I calculation.

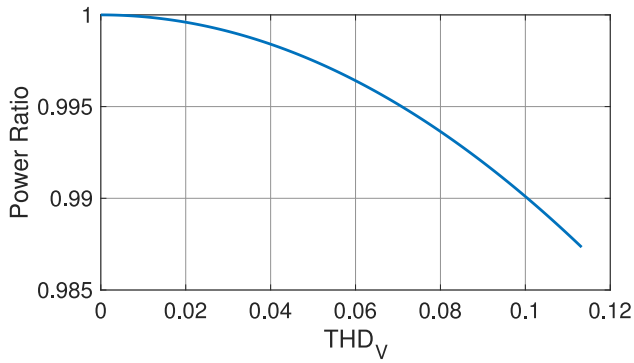

Fig. 1. Power ratio of the fundamental active power with respect to the total power for a linear load for different THD values.

A. Linear Load

Under the assumption of a linear load the THD_I is equal to the THD_V. This means that the values from Table I are chosen for both the current and the voltage. Taking the worst case allowed values for every single harmonic, a maximum THD_V of 0.11 is found. This is even higher than the accepted supply voltage THD_V of 0.08 as specified in EN 50160. All THD values up to 0.11 are considered for both the current and the voltage following the same ratio from Table I. For all these different THD values, the power ratio of the fundamental active power with respect to the total power delivered to the linear load is calculated. This result can be seen in Fig. 1, for which THD_I equals the THD_V, due to the linear load. Different combinations of THD_V and THD_I would show the effect of nonlinear loads on the amount of active power in the fundamental frequency components with respect to the total power, which will be elaborated on.

It is important to note that even with a THD of 0.11 for both the voltage and the current, more than 98% of the total power coincides in the fundamental frequency component. This raises the attention about shifting our focus away from the higher frequency components and more toward the fundamental active power. Furthermore, under the assumption of a pure sinusoidal supply voltage the THD_I has no effect on the average active power, regardless of the frequency components in the current, and thus it is sufficient to only consider the fundamental active power.

B. Nonlinear Load

The orthogonality of power flow toward a nonlinear load is considered using the limits of IEC 61000-3-2 for Class C equipment, as stated in Table II. The worst case THD_I following these values is 0.34. Again all the THD values are investigated following the same ratio from zero until the worst allowable distortion, for both the voltage (EN 50160) and the current (IEC 61000-3-2). The fundamental active power with respect to the total power in the nonlinear load is calculated and can be seen in Fig. 2.

The flat line of 1 at a THD_V of zero shows that a perfect energy measurement result is achieved when only considering the fundamental active power, regardless of the intensity of

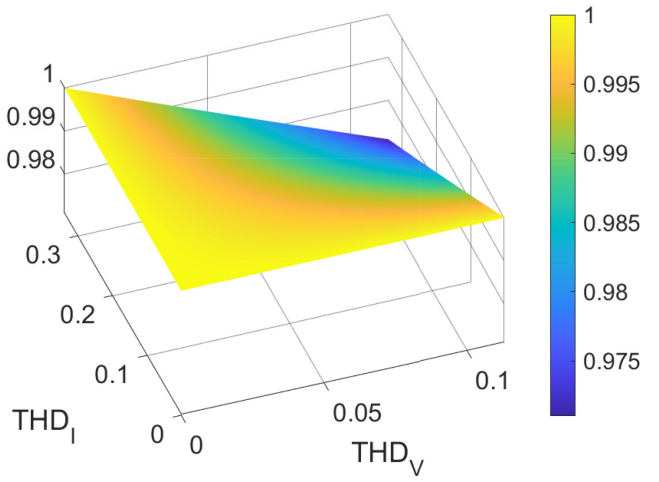

Fig. 2. Power ratio of the fundamental active power with respect to the total power for a nonlinear load for different THD_V and THD_I values.

THD_I, since the nonfundamental active power is zero. In other words, if the wideband current signal in an energy meter would be fitted with a basic low-pass filter, the active power and energy measured would be exactly the same as when the, even extreme wideband, current signal would be used without a filter. The results in Fig. 2 show that even at the worst-case scenario of a THD_V of 0.11 supplied by the grid and a THD_I of 0.34, the power calculation using only the fundamental active power has an error of less than 2.5% compared to the total power considering all components. This error is within the maximum permissible error limit for electricity meters used in Europe with approval of the European measuring instrument directive and according to the European standard EN 50470-3:2006 [27].

IV. Measurement Setup I—DC

To verify the feasibility of the orthogonality concept, a programmable load is used in combination with a Keysight E36234 A voltage source set to 10 V dc. The load is programmed to vary "sinusoidally," between 0.5 and 1.5 A. The resulting voltage and current waveforms can be seen in Fig. 3(a).

In the figure one can clearly distinguish the dc behavior in the voltage versus the dc plus sinusoidal behavior of the current. The active power that will actually be consumed is due to the dc component in the current. The 50 Hz component of the current will deliver no work and is therefore of no importance when one is interested in the actual active power of the load. To emphasize on the difference in frequency components, their respective frequency plots can be seen in Fig. 3(b).

For this case, it seems trivial that the extra frequency component in the current adds nothing to the active power. Instantaneous power shows a higher current flow through the load during the first-half of the 50 Hz sinusoidal period, while in the other-half of the period, it is vice versa and thus resulting in a zero average contribution to the active power consumed. This physically results in the load warming up and cooling down over time, with respect to the average power when not considering this

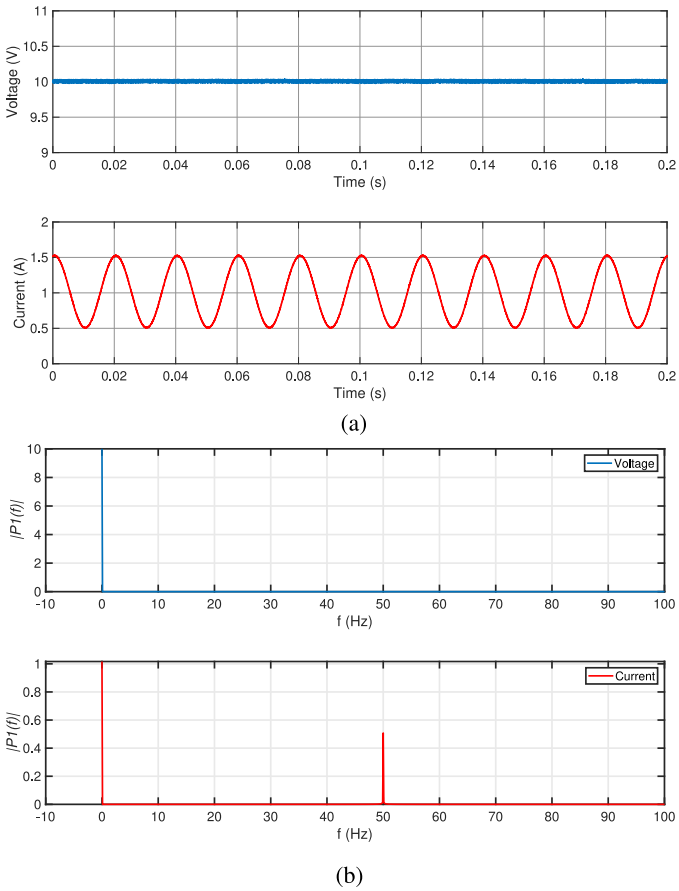

Fig. 3. Voltage (blue) and current (red) measured at the output of the dc source. (a) Time domain. (b) Single-sided amplitude spectra of the voltage and current.

extra frequency component in the current. This case is extended in the following section to an ac voltage source, where the current also has additional harmonics that do not occur in the voltage waveform. When considering energy measurements low-pass filter elements should be used to decrease the susceptibility to high-frequency harmonics caused by the nonlinear currents.

V. Measurement Setup II—Pure 50 Hz

To emphasize orthogonal power flow occurring in ordinary situations a full wave rectifier has been used, which can be found in many COTS equipment. It is well known that a full wave rectifier introduces harmonics in the current [28]. The rectifier is followed by a capacitor in parallel with a resistor. For these measurements, a 70.71 V_{rms} ideal, i.e., nondistorted, sinusoidal voltage is generated using a four-quadrant pacific power smart source 140-TMX AC. This ideal nondistorted sinusoidal voltage results in a single frequency component with a peak voltage of 100 V. In the following sections, peak values are used to represent the individual sinusoidal component of the voltage and current waveform to better relate the mentioned values to the frequency graphs.

The test setup that is used is shown in Fig. 4. A dc electronic load (BK8601) is used to sink all the dc current generated by the

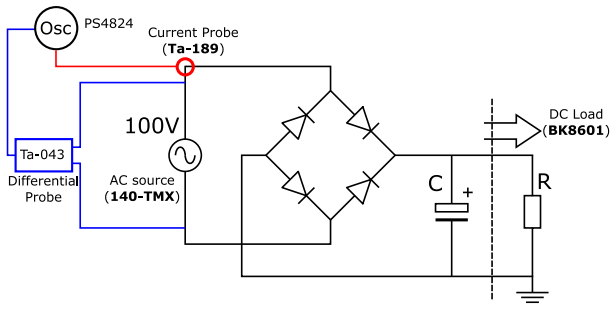

Fig. 4. Schematic overview of the measurement setup with a rectifier test case.

circuit. The BK8601 is programmable and gives a measurement of the power that is being dissipated. This programmable electronic load has a maximum dc voltage rating of 120 V. Because of this constraint, the supply voltage is set to 70.71 V_{rms} with a peak value of 100 V in order to protect the equipment. Using a 220 μF capacitor and 1 $k\Omega$ load resistance will result in a voltage ripple of approximately 5% at the load. The rectifier starts conducting twice in the 50 Hz period causing the capacitor to charge via a current pulse, causing harmonic distortion in the current waveform.

This measurement setup emulates a common situation, where higher frequency components in the form of harmonics are created in the current, while the voltage remains 50 Hz. Measurements are performed with a multichannel digitizer, in this case, a PicoScope PS4824. The current and voltage waveforms measured at the output of the source are shown in Fig. 5(a). It can be clearly seen that the voltage is mainly sinusoidal, while the current is impulsive. Based on Fourier analysis, the impulsive current constitutes of many uneven, higher harmonics. The frequency content of both signals has been plotted in Fig. 5(b). The active power consumed by the load corresponds to 9 W, which is mainly due to the 0.18 $A_{Pk,\,50\,Hz}$ and 100 $V_{Pk,50\,Hz}$ of the 50 Hz component. Even though the fact that the higher harmonics in the current have almost the same amplitude as the 50 Hz component, they add almost nothing to the active power being consumed. When considering energy measurements a low-pass filter should be used to reduce the EMI caused by the nonlinear currents and the corresponding higher frequency harmonics. In this article, we have looked at the extreme case of only taking the 50 Hz component into account, while still remaining within the measurement accuracy limits for electricity meters.

This measurement shows that when a grid is maintained without any significant harmonic distortion, active power measurements can be confined to the very low frequencies, i.e., the fundamental supplying frequency. This allows for measurement circuit design, which is very robust against high-frequency current harmonics, for instance by employing basic low-pass filters.

VI. Measurement Setup III—Adding Harmonics

The effect of harmonics, representing actual power supply grids, is demonstrated in this section. Using the pacific power

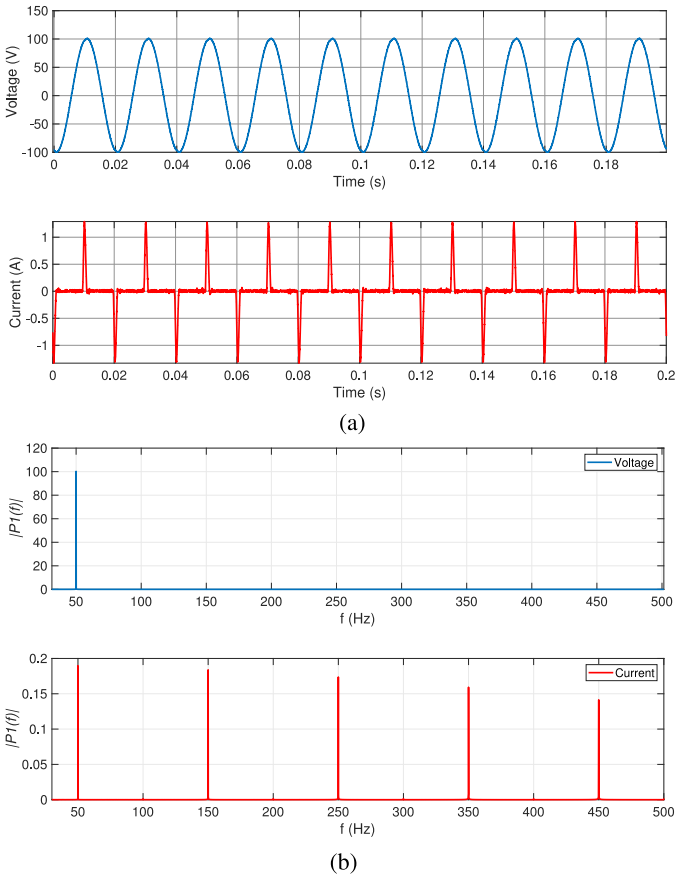

Fig. 5. Voltage (blue) and current (red) measured at the output of the source during the diode rectifier setup. (a) Time domain. (b) Single-sided amplitude spectra of the voltage and current.

smart source 140-TMX AC, a 50 Hz grid is emulated with an additional third harmonic. Due to the phase, the harmonic can be added destructively, i.e., creating a lower peak in the voltage, and constructively, i.e., increasing the peak of the voltage [1]. The fundamental component is 100 $V_{Pk,\,50\,Hz}$, while the third harmonic is 10% of the fundamental component (10 $V_{Pk,\,150\,Hz}$). A relatively high value for the third harmonic, outside the EN 50160 limits, is chosen to emphasize the importance of keeping the grid voltage within the allowable distortion levels w.r.t. EN 50160. In this example, a significant power of around 5% can be found in the third harmonic when not adhering to the limits. This extra frequency component does also influence the functionality of the load, and therefore the power flow within the load. The measurement for this apparent power, however, remains completely orthogonal, i.e., the 150 Hz component is not involved with the 50 Hz component for the active power measurement.

A. Destructive Harmonics

Based on the theory of orthogonal power flow, it is expected that the third harmonic will add active power to the system and thus increase the total power consumption. The assumption here is that the current drawn by the load is unaffected by the change in voltage supply. However, it turned out, after measuring a lower

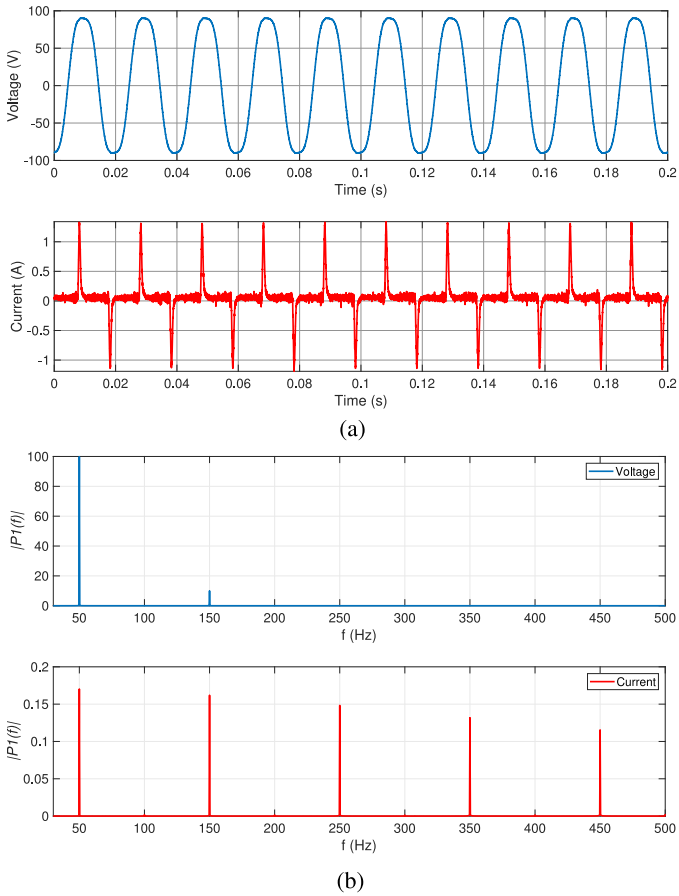

Fig. 6. Voltage (blue) and current (red) measured at the output of the source with destructive harmonics added to the voltage. (a) Time domain. (b) Single-sided amplitude spectra of the voltage and current.

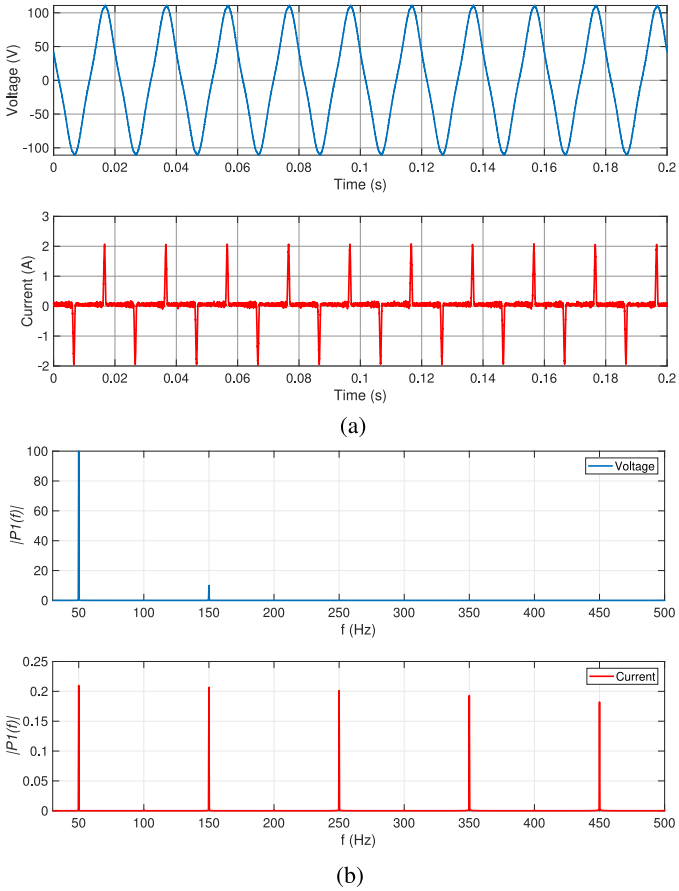

Fig. 7. Voltage (blue) and current (red) measured at the output of the source with constructive harmonics added to the voltage. (a) Time domain. (b) Single-sided amplitude spectra of the voltage and current.

power consumption, that the current drawn was lower. This can be seen by comparing Fig. 6 with Fig. 5, as the voltage waveform has a lower peak. This can be explained, by the negative peak of the 150 Hz coinciding with the positive one of the 50 Hz, lowering the maximum voltage peak, thus lowering the average voltage of the capacitor and inherently lowering the current drawn by the resistor.

B. Constructive Harmonics

When phase shifting the 150 Hz harmonic 180° with respect to itself, the harmonic interference adds constructively at the top of the 50 Hz voltage increasing the maximum peak of the total voltage as seen in Fig. 7(a), while again keeping the 50 Hz component constant at 70.71 V_{rms}, see Fig. 7(b).

It is important to emphasize on the fact that these harmonics in the grid can hugely affect the function of equipment in a household. Either lowering the power consumed in such a way that the equipment does not turn-ON anymore, or increasing it such that the equipment can even break down. However, it is key to emphasize here that the orthogonality of power flow is maintained. There is no interaction between voltage of one frequency in combination with a current on another. In this example, a significant power can be found in the third harmonic. This is due to the fact that the third harmonic of the voltage is outside the EN 50160 limits and the current also has high harmonics not falling within the Class C equipment standard. The functionality of the equipment itself, does effect the total active power. In the measurement case, a reduction or increase in active power is purely due to the reduced and increased dc voltage provided to the resistance.

VII. Overview

A schematic overview of this article is given in Fig. 8, showing the difference between a static energy meter, with and without a basic low-pass filter. This figure is divided in three separate parts, first it shows that no errors occur for both cases in an ideal situation with no THD for both the voltage and the current. In the middle section, it shows that a static energy meter without a low-pass filter is prone to errors due to THD_I. The static energy meter with a low-pass filter, however, still shows perfect results. The last scenario, with a THD for both the voltage and current, shows an error prone static energy meter without a low-pass filter. The static energy meter with a low-pass filter remains within limits, as considered for Class C equipment [23].

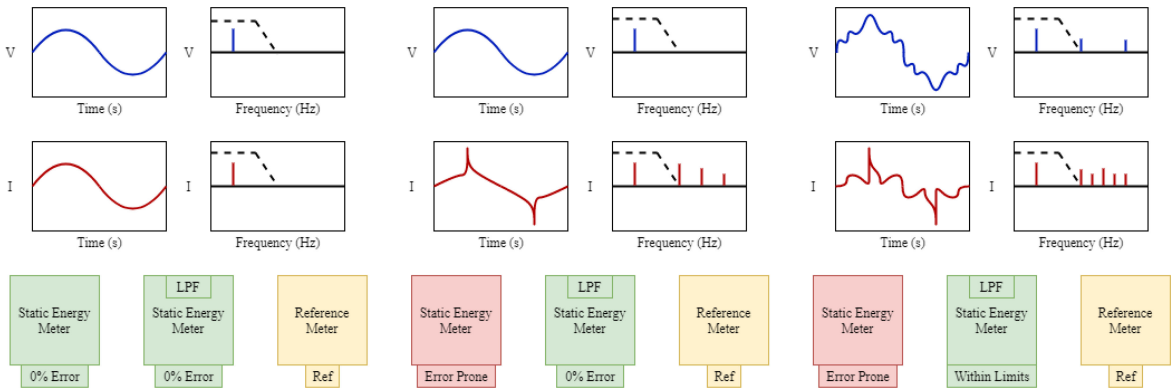

Fig. 8. Left: Pure 50 Hz voltage and current, Middle: Pure 50 Hz voltage and a current with THD, Right: THD for both the voltage and current.

VIII. Conclusion

In this article, a theoretical model, simulations and measurements were presented to prove that for reliable energy measurements, only the fundamental 50 Hz component of the current should be considered if the voltage source is a pure 50 Hz. Also, in case of a THD_v of 0.11 and a THD_i of 0.33, as a worst case allowed scenario following the international standards EN 50160 and IEC 61000-3-2 for Class C equipment, more than 97.5% of the total power is still confined to the fundamental frequency. Thus, by filtering the harmonics, created by nonlinear loads, a reliable active power and energy measurement can be performed, and no high sampling of the current waveform is needed. The trend toward measuring active power up to higher frequencies does not add significant improvements to the accuracy of the total power measurement, while it adds unnecessary complexity and electromagnetic susceptibility. Two measurement setups were used to validate the theoretical model. A dc source was loaded with a variable impedance, introducing higher frequency components in the current, which did not contribute to the registered average dissipated power. A more common case of using a diode rectifier connected to an ac voltage supply, showed similar results. The harmonics in the current do not add any active power to the load, if the voltage source quality is maintained, i.e., no harmonic distortion. Finally, it was shown that adding harmonics in the voltage can influence the power drawn by the load. However, the total active power can still be determined via the orthogonality principle and thus measuring only at the fundamental frequency.

Acknowledgment

The results found reflect the author's view only. EURAMET is not responsible for any use that may be made of the information it contains.

References

[1] T. H. Ortmeyer, K. R. Chakravarthi, and A. A. Mahmoud, "The effects of power system harmonics on power system equipment and loads," *IEEE Trans. Power App. Syst.*, vol. PAS-104, no. 9, pp. 2555–2563, Sep. 1985.

[2] R. B. Timens, F. J. Buesink, V. Ćuk, J. F. Cobben, W. L. Kling, and F. B. Leferink, "High harmonic distortion in a new building due to a multitude of electronic equipment," in *Proc. IEEE Int. Symp. Electromagn. Compat.*, pp. 393–398, 2011.

[3] L. Cividino, "Power factor, harmonic distortion: Causes, effects and considerations," in *Proc. 14th Int. Telecommun. Energy Conf.*, 1992, pp. 506–513.

[4] N. Oswald, P. Anthony, N. McNeill, and B. H. Stark, "An experimental investigation of the tradeoff between switching losses and EMI generation with hard-switched All-Si, Si-SiC, and All-SiC device combinations," *IEEE Trans. Power Electron*, vol. 29, no. 5, pp. 2393–2407, May 2014.

[5] R. B. Timens, "Electromagnetic Interference of Equipment in Power Supply Networks," Ph.D. Dissertation, Univ. Twente, Enschede, The Netherlands, 2013.

[6] M. Bollen, A. Castro, and S. Rönnber, "Typical harmonic levels and spectra with low-voltage customers," in *Proc. 25th Int. Conf. Electricity Distrib. – CIRED*, Madrid, 2019, pp. 1–5.

[7] V. Ćuk, J. F. G. Cobben, W. L. Kling, and R. B. Timens, "An analysis of diversity factors applied to harmonic emission limits for energy saving lamps," in *Proc. 14th Int. Conf. Harmon. Qual. Power*, Sep. 2010, pp. 1–6.

[8] M. J. H. Rawa, D. W. P. Thomas, and M. Sumner, "Factors affecting the harmonics generated by a cluster of personal computers," in *Proc. 16th Int. Conf. Harmon. Qual. Power*, May 2014, pp. 167–171.

[9] "Electromagnetic compatibility (EMC) - Part 4-30: Testing and measurement techniques - Power quality measurement methods," no. TC 77/SC 77A, 2015.

[10] M. Bollen, M. Olofsson, A. Larsson, S. Rönnberg, and M. Lundmark, "Standards for supraharmonics (2 to 150 kHz)," *IEEE Electromagn. Compat. Mag.*, vol. 3, no. 1, pp. 114–119, Jan.–Mar. 2014.

[11] "Yokogawa Power Analyzers and Power Meters," Accessed: Mar. 17, 2020. [Online]. Available: https://tmi.yokogawa.com/solutions/products/power-analyzers/

[12] "Hioki High Precision Power Meters | Power Analyzers," Accessed: Mar. 3, 2020. [Online]. Available: https://www.hioki.com/en/products/list/?category=15

[13] "Newtons4th Power Analyzers," Accessed: Mar. 3, 2020. [Online]. Available: https://www.newtons4th.com/products /power-analyzers

[14] F. Leferink, C. Keyer, and A. Melentjev, "Runaway energy meters due to conducted electromagnetic interference," in *Proc. Int. Symp. Electromagn. Compat.*, Wroclaw, 2016, pp. 172–175.

[15] F. Leferink, C. Keyer, and A. Melentjev, "Static energy meter errors caused by conducted electromagnetic interference," *IEEE Electromagn. Compat. Mag.*, vol. 5, no. 4, pp. 49–55, Oct.–Dec. 2016.

[16] C. Keyer and F. Leferink, "Conducted interference on smart meters," in *Proc. IEEE Int. Symp. Electromagn. Compat. Signal/Power Integrity*, 2017, pp. 608–611.

[17] B. ten Have, T. Hartman, N. Moonen, C. Keyer, and F. Leferink, "Faulty readings of static energy meters caused by conducted electromagnetic interference from a water pump," in *Proc. Int. Conf. Renew. Energies Power Qual.*, 2019, pp. 15–19.

[18] Z. Marais, H. E. V. D. Brom, G. Rietveld, R. V. Leeuwen, D. Hoogenboom, and J. Rens, "Sensitivity of static energy meter reading errors to changes in non-sinusoidal load conditions," in *Proc. Int. Symp. Electromagn. Compat.*, 2019, pp. 202–207.

[19] *Electromagnetic Compatibility (EMC) Part 4-11: Testing and Measurement Techniques-Voltage Dips, Short Interruptions and Voltage Variations Immunity Tests*, Standard IEC 61000-4-11:2004/AMD1:2017(E), 2017.

[20] P. S. Wright *et al.*, "Evaluation of EMI effects on static electricity meters," in *Proc. Conf. Precision Electromagn. Meas.*, 2018, pp. 1–2.
[21] B. ten Have, T. Hartman, N. Moonen, and F. Leferink, "Inclination of fast changing currents effect the readings of static energy meters," in *Proc. Int. Symp. Electromagn. Compat.*, 2019, pp. 208–213.
[22] *Voltage Characteristics of Electricity Supplied by Public Electricity Network*, Standard CENELEC – EN 50160, 2010.
[23] *Electromagnetic Compatibility (EMC) – Part 3-2: Limits – Limits for Harmonic Current Emissions (Equipment Input Current ≤16 A Per Phase*, Standard NEN-EN-IEC 61000-3-2:2018, 2018.
[24] J. A. Ferreira, "The multilevel modular DC converter," *IEEE Trans. Power Electron.*, vol. 28, no. 10, pp. 4460–4465, Oct. 2013.
[25] L. Peretto, J. Willems, and A. Emanuel, "The effect of the integration interval on the measurement accuracy of rms values and powers in systems with nonsinusoidal waveforms," in *Proc. IEEE Int. Workshop Appl. Meas. Power Syst.*, 2007, pp. 47–52.
[26] *IEEE Standard Definitions for the Measurement of Electric Power Quantities Under Sinusoidal, Nonsinusoidal, Balanced, or Unbalanced Conditions*, IEEE Standard 1459-2010 (Revision of IEEE Std 1459-2000), 2010, pp. 1–50.
[27] *Electricity Metering Equipment (a.c.) – Part 3: Particular Requirements – Static Meters for Active Energy (Class Indexes A, B and C)*, Standard EN 50470-3:2006/A1:2018, 2018.
[28] A. Mansoor, W. M. Grady, R. S. Thallam, M. T. Doyle, S. D. Krein, and M. J. Samotyj, "Effect of supply voltage harmonics on the input current of single-phase diode bridge rectifier loads," *IEEE Trans. Power Del.*, vol. 10, no. 3, pp. 1416–1422, Jul. 1995.

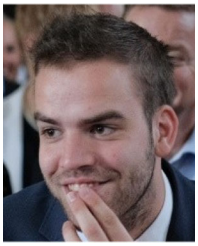

Tom Hartman received the bachelor's and the master's degrees in electrical engineer in 2016 and 2018, respectively, from Telecommunication Engineering Group, University of Twente, Enschede, The Netherlands, where he is currently working toward the Ph.D. degree in electromagnetic compatibility.

He is currently working on a project about electromagnetic interference on static electricity meters. In this project, he works on improving the digital signal processing techniques used for multichannel TDEMI measurements.

Roelof Grootjans received the M.Sc. degree in electrical engineering from Telecommunications Group, the Univeristy of Twente, Enschede, The Netherlands, in 2016.

Since then, he has been working with the small company that develops explosive trace detection equipment using ion mobility spectrometry. Since august 2019, he has been working as a Technician with the University of Twente to support lab activities and electronics development related to electromagnetic compatibility and power electronics.

Niek Moonen (Member, IEEE) received the B.Sc. degree in advanced technology, the M.Sc. degree in electrical engineering, and the Ph.D. (*Cum Laude*) degree in electromagnetic compatibility and from the University of Twente, Enschede, The Netherlands, in 2012, 2014, and 2019, respectively.

His research interests include EMI mitigation in power electronics with special interest in EMI propagation in smart grids, digital signal processing in EMC measurements, and EMI filter optimization.

Dr. Moonen is the member of IEEE EMC society TC7 on low-frequency EMC and board member of the Dutch EMC-ESD association.

Frank Leferink (Fellow, IEEE) received the B.Sc., M.Sc., and Ph.D. degrees in electrical engineering from the University of Twente, Enschede, The Netherlands, in 1984, 1992, and 2001, respectively.

He has been with THALES in Hengelo, The Netherlands, since 1984 and is currently with the Technical Authority EMC. He is also the Manager of the Network of Excellence on EMC with the THALES Group, with more than 100 EMC engineers scattered over more than 20 units, worldwide. In 2003, he was appointed as Part-Time Professor and Full Research Chair for EMC with the University of Twente. At the University of Twente, he lectures the course EMC, and manages several research projects, with two researchers and 15 Ph.D. student-researchers. More than 300 papers have been published at international conferences or peer reviewed journals, and he holds 5 patents.

Prof. Leferink is the Past-President of the Dutch EMC-ESD association, Chair of the IEEE EMC Benelux Chapter, member of ISC EMC Europe, Chairman of EMC Europe 2018 (Amsterdam), member of the Board of Directors of the IEEE EMC Society, and Associate Editor for the IEEE TRANSACTIONS ON ELECTROMAGNETIC COMPATIBILITY and the IEEE LETTERS ON ELECTROMAGNETIC COMPATIBILITY PRACTICE AND APPLICATIONS.